MECHANICAL STRUCTURAL ANALYSIS
AND
DESIGN OPTIMIZATION
OF
INDUSTRIAL ROBOTS

Felix Hou

Clarence DeSilva

Paul Wright

Table of Contents

SUMMARY

In an automated Flexible Machining Cell an Industrial Robot is required to carry out loading and off-loading tasks and participate in off-line measurement. In these activities the robot speed, accuracy and compliance are the important performance measures. Improvement in speed reduces overall job time but this is generally achieved at the expense of accuracy. A further trade-off is that of weight-lifting capability and accuracy. It is well known that commercial robot suppliers provide a range of machines in which accuracy is lost as speed is increased.

This report summarizes some progress to date of basic research on the mechanical structural analysis and control of an industrial robot. The research is addressing this speed vs. accuracy vs. load capacity trade-off. To improve the robot performance a mathematical model of the robot dynamics is desirable. The model developed relates to a Trallfa robot but the results are applicable to other machines.

The initial set of model equations are highly non-linear, time variant and coupled. Thus model reduction has been applied in which the gravitational fore components in each joint in the static mode have been separated out. In addition the base rotation has been developed from the rest of the system. The research results suggest that the third link should be heavily built to offset the gripper loading effect.

1 INTRODUCTION

The existing industrial robots can be divided into three categories according to their control equipment [1];

- point-to-point type

- limited-sequence type

- continuous-path controlled type.

The first category, point-to-point, is the simplest. The robots in this category are usually built for pick-and-place type of jobs in a highly structured environment. The motions involved here are back-and-forth between two end points. The actuators move the robot joints from one position to the other and the motion is stopped either by a limit switch or by some mechanical stop devices. The position accuracy is guaranteed by the stop devices. The robots in this category are usually very fast and accurate.

The second category, limited-sequence machine, is the natural extension of the point-to-point type. The robot in this category moves along a space trajectory which is specified by multiple set-points. The robot moves from a set-point to the next set-point, and then to the next..etc. The joint coordinates at those set-point are pre-calculated and stored in the memory. Each joint is controlled by an independent position servo and all joints move from position to position independently. When all joints have reached a set point, then they start approaching to the next. Servo gains can be adjusted independently by the operator, and the motions can be optimized to any given task. The limited-sequence machine is fast, but its motion is uncoordinated in the sense that the trajectory between set-point is not controlled. Further, as the individual servo gains are adjusted, the path described in space changes. The robot in this category can be used for "gross motion", in which the path of the end-effector does not matter [2].

For more advanced applications, like parts assembling, the path between adjacent set points must also be controlled [3]. The continuous path controlled robot is capable of coordinated motion from point to point along the path. An example is the Cincinnati Milacron's T3 robot [4,5] in which all motions of the end-effector are along straight lines with controlled acceleration and deceleration. Unfortunately these motions require constant mathematical transformation between cartesian coordinates of the end-effector to joint actuator coordinates in order to control the robot [6,7].

The control of the robot manipulator is essential to the robot performance. In the analysis of a manipulator, two problems are encountered. The first, called the positioning problem, can be stated as follows: 'Given the desired position and orientation of the free end of the manipulator, what are the

joint positions (angles) which will position the free end at the desired point in space with the specific orientation' This is a kinematic problem and it had been studied by Pieper [8]. The second problem is one of the manipulator dynamics and control. It can be stated as follows: 'Given the initial and final positions of the end-effector, how should each joint move from the initial to the final position'

2 MANIPULATOR DYNAMICS AND CONTROL

The manipulator is in effect a multiple degree of freedom chain linkage with a joint between each linkage pair. Each joint must change its coordinate in order to position the end-effector at the right place. If each joint moves from initial to final position independently, the trajectory of the free end is uncoordinated. For example, a two dimensional motion from point A to point B is shown in figure 1. It can be seen that different servo gains for X axis and Y axis will cause different trajectories. If a particular path (say a straight line from A to B) is to be followed, then the joints must be driven in a constraint manner. Obviously, an algorithm is needed to correlate the motion of each individual joint. This algorithm is basically the mathematics of homogeneous coordinate transformation. If the speed of each joint is constrainted in some manner, the motion is called coordinated motion. The practical difficulty with the coordinate transformation approach is that it involves too many trajectory calculations. In a real-time environment, the existing mini/micro computers simply do not have enough computing power to finish the calculation in the required time frame. There are a number of ways to handle this difficulty;

1. A multiprocessor computer system with dedicated CPU for the calculations. Other CPUs can be used to handle general I/O and servo loop control.

2. A hierarchical controller structure is proposed by Albus [9]. A high level minicomputer is used for trajectory calculation. A low level microcomputer receives the results of that calculation from a 'shared memory', and in term controls each servo loop.

3. Anderson [10] suggests an easier way to implement a coordinated motion without the transformation calculation. The speed of movement is also improved. But the trajectory is not a straight line between two set points, though it is predictable.

There are some studies about the manipulator control reported in the literature [11, 12, 13]. Most of these advanced control schemes do not consider a coordinated motion. Two of them are cited here.

In reference [11], a multi-structure-system (VSS) approach for controlling a hexapod locomotion is presented. The plant under computer control is a hexapod. There are 6 legs mounted on this unit, each leg is composed of 3 articulated linkages powered with electric motors. The motors are regulated by phase angle control which has well known nonlinearity. The friction between moving parts varies widely during operation. Loading has a substantial effect on the system dynamics. All in all, such a non-linear system is nearly impossible to model, even empirically, and is a prime candidate for the sliding mode method.

Sliding mode control, an example of a variable structure system (VSS), is designed so that the system operates on a preassigned trajectory in the phase plane, and thus becomes insensitive to external influences. The entire group of variable structure control system is characterized by discontinuous switching between different control laws depending on the state of the system.

In the cited example, the phase plane is formed by joint position error 0err vs. its angular velocity 9. A sliding line S = 0 is decided to be:

$$S = -C0err + \dot{9}$$

where C<0. The sliding line S = 0 and the Y axis divides the phase plane into two pairs of regions; namely, define Region 1 to be where 0errS>O and define Region 2 to be where 8errS<0. ©errS is the switching condition. The VSS decision rule is to apply different control laws in Region 1 and Region 2. Two sets of control laws, opposing each other, are implemented; these are

$$V= Sgn(0err) */^ + y^err \quad Region \ 1$$

$$= Sgn(Gerr) * fi_2 + y_20err \quad Region \ 2$$

where $p^\wedge \ P_2 \ y_1 \ y_2$ are the controller parameters. V is the voltage to the driving motor. The effect of the first control law, with $y_1 = 0>$ k shown in figure 2b. The effect of the second control law, with $y_2 = f\$_2 = 0$ is shown in figure 2c. It can be seen, figure 2d, that once the system reaches the line S = 0, it will "slide" along the line toward the origin, assuming that the switching between control laws can be done at infinite frequency. The existance of a sliding mode is guaranteed by having both the control laws forcing the state of the system toward the line S = 0. Once the system is in the sliding mode, then its motion is described by:

$$©err(t) = \theta err(0)e^{ct}$$

which depends on parameter C only. Therefore the sliding mode method is intrinsically insensitive to the unit's parameter variations and interaction effects with other links.

In reference [12], another novel approach is presented to control a six«degree-of-freedom robot arm. The use of conventional linear control techniques limits the basic dynamic performance of manipulators in a number of ways. Two of these which are very significant are

1. The dynamic characteristics of general spatial manipulators which are highly nonlinear functions of the positions and the velocities of the manipulator elements.

2. The degradation of the dynamic performance of the manipulator by the inertia! properties of the objects being manipulated.

In view of these drawbacks, Model-Reference-Adaptive-Control (MRAC) is introduced to attack the nonlinear, time varing system. The basic ideal behind MRAC is to force the system characteristics to be the same as that of a reference model, by means of nonlinear compensation. In figure 3, tie plait

output is compared with the reference model output. The difference E, is used to drive an adaptive mechanism, which in turn adjusts the plant feedback gains such as to minimize the error signal E. The theory of MRAC is beyond the intention of this report, however the method applied in this cited example is probably the simplest among all MRAC implementations. An excellent reference about the theoretical background is in [14].

3 ROBOT MODEL DEVELOPMENT

The investigation of these manipulator control strategies is an essential aspect of improving manipulator accuracy for such applications as automated inspection of turbine blades. A useful way of comparing rival control strategies is modelling of the mechanical system.

The robot under consideration is depicted in Figure 4. It is of fairly general type, with 3 linkages for the arm connected by 3 rotary joints. The first link rotates with respect to a vertical axis from the fixed robot base. It simulates the waist motion of a human body. The second link rotates along a horizontal axis which passes through the tip of the first link. This motion is similar to that provided by the human shoulder. The third link rotates along a horizontal line at the tip of the second link. This link is the elbow of the robot arm system. With these 3 links and 3 rotary joints, this robot is of 3 degree of freedom, and is capable of putting the gripper to any location in its reachable working environment. The orientation of the gripper is handled by the gripper actuator, which is a 3 degree of freedom device in itself. It should be pointed out that the gripper, or the hand, is not included in the current manipulator model.

The first step towards the present model of the robot is to derive the equations of motion. In ths work, the equations of motion are derived from the fundamental principles of force-moment balance. There are similar robot models reported in the literature [1]. However, all of these previous investigations were done by the Lagrangian (energy) approach. The reactional force and moment at each joint may be more useful from the viewpoint of the mechanical structure analysis and design optimization.

Within the scope of a vectorial approach, the D'Alembert method has been chosen to formulate the problem for its simplicity and clarity. The D'Alembert principle can be stated as follows;

.....Since the product of mass and acceleration is equivalent to force, a body possessing acceleration could be considered to be in "equilibrium" under the action of a hypothetical inertia force whose mangitude is M*A and whose direction is opposite to that of the acceleration A.

According to the method outlined above, a kinematic analysis is performed to find out the absolute acceleration for any point (actually a small element of mass) on the robot arm (Appendix A). Once the

acceleration is known, then the inertia force can be calculated by F = M*A and can be applied to oppose the acceleration. If so done, the robot dynamics becomes a static problem and the equilibrium equations can be easily derived. These equilibrium equations are solved in a reverse order; the third link first, then the second link, then the first link (Appendix B).

It is desirable to put the equations of motion thus derived into a state-space form to facilitate the further analysis and computer simulation. For the robot system under consideration, it is natural to choose the angles of the rotary joints and the rates of change (angular velocities) as the state variables. However, this attempt is not successful, due to the square terms and the cross-coupling between the angular velocities. The result of this attempt is given below;

$$
\begin{aligned}
\{I_1 &+ m_2 l_1^2 + m_3 l_1^2 + I_3 \sin^2(\theta_2 + \theta_3) + (I_2 + m_3 l_2^2)\cos^2\theta_2 \\
&+ 2l_1(m_2 c_2 + m_3 l_2)\cos\theta_2 + 2m_3 l_1 c_3 \sin(\theta_2 + \theta_3) \\
&+ 2m_3 l_2 c_3 \cos\theta_2 \sin(\theta_2 + \theta_3) \quad \}\ddot{\theta}_1 = T_1 +
\end{aligned}
$$

$$
\begin{aligned}
\dot{\theta}_1 \dot{\theta}_2 \{ &2[m_2 l_1 c_2 + m_3 l_1 l_2 + (I_2 + m_3 l_2^2)\cos\theta_2]\sin\theta_2 \\
&-2m_3 l_2 c_3 [\cos\theta_2 \cos(\theta_2 + \theta_3) - \sin\theta_2 \sin(\theta_2 + \theta_3)] \\
&-2[m_3 l_1 c_3 + I_3 \sin(\theta_2 + \theta_3)]\cos(\theta_2 + \theta_3) \quad \}-
\end{aligned}
$$

$$
\dot{\theta}_1 \dot{\theta}_3 \{ 2m_3 c_3 (l_2 \cos\theta_2 + l_1)\cos(\theta_2 + \theta_3) + 2I_3 \sin(\theta_2 + \theta_3)\cos(\theta_2 + \theta_3) \} \tag{1}
$$

$$
\begin{aligned}
\{(I_2 + m_3 l_2^2)I_3 &- m_3^2 l_2^2 c_3^2 \sin^2\theta_3 \}\ddot{\theta}_2 = I_3 T_2 - (I_3 + m_3 l_2 c_3 \sin\theta_3)T_3 \\
&-(m_2 c_2 + m_3 l_2)g I_3 \cos\theta_2 + (m_3^2 l_2^2 c_3^2)g \sin(\theta_2 + \theta_3)\sin\theta_3 \\
&-\dot{\theta}_1^2 \{[m_2 I_3 l_1 c_2 + m_3 I_3 l_1 l_2 + (I_2 I_3 + m_3 I_3 l_2^2)\cos\theta_2 + m_3 I_3 l_2 c_3 \sin(\theta_2 + \theta_3)]\sin\theta_2 \\
&\quad + [m_3^2 l_1 l_2 c_3^2 + m_3^2 l_2^2 c_3^2 \cos\theta_2 + m_3 I_3 l_2 c_3 \sin(\theta_2 + \theta_3)]\sin\theta_3 \cos(\theta_2 + \theta_3) \quad \} \\
&-\dot{\theta}_2^2 \{m_3 l_2 c_3 (I_3 + m_3 l_2 c_3 \sin\theta_3)\cos\theta_3 \} \\
&-\dot{\theta}_3^2 \{m_3 I_3 l_2 c_3 \cos\theta_3 \} \\
&-\dot{\theta}_2 \dot{\theta}_3 \{2m_3 I_3 l_2 c_3 \cos\theta_3 \} \tag{2}
\end{aligned}
$$

$$
\begin{aligned}
\{(I_2 + m_3 l_2^2)I_3 &- m_3^2 l_2^2 c_3^2 \sin^2\theta_3 \}\ddot{\theta}_3 = \{-(I_3 + m_3 l_2 c_3 \sin\theta_3)\}T_2 \\
&+ \{I_2 + I_3 + m_3 l_2^2 + 2m_3 l_2 c_3 \sin\theta_3 \}T_3 \\
&+ \{(m_2 I_3 c_2 + m_2 m_3 l_2 c_2 c_3 \sin\theta_3 + m_3 I_3 l_2 + m_3^2 l_2^2 c_3 \sin\theta_3)g \cos\theta_2
\end{aligned}
$$

$$-m_3c_3(m_3l_2^2 + I_2 + m_3l_2c_3\text{sine}_3)g\,\sin(G_2 + \theta_3)\ \}$$

$$+\dot\theta_1^2\{[m_2I_3l_1c_2 + m_3I_3l_1l_2 + (I_2I_3 + m_3I_3l_2^2)\cos\theta_2 + m_2m_3l_1l_2c_2c_3\sin\theta_3$$

$$+\ m_3^2l_1^2l_2c_3\text{sine}_3 + m_3I_2l_2c_3\sin\theta_3\cos\theta_2 + m_3^2l_2^3c_3\sin\theta_3\cos\theta_2]\sin\theta_2$$

$$+\ [m_3^2l_1l_2c_3^2\sin\theta_3 + (I_2I_3 + m_3I_3l_2^2 + m_3I_3l_2c_3\sin\theta_3)\sin(\theta_2 + \theta_3) +$$

$$m_A\cdot_1c_3 + m_{\wedge 2}l_2c_3\cos e_2 + m_{3>1}^2l_2^2c_3 + m_3^2l_2^3c_3\cos\theta_2\quad]\cos(\theta_2 + \theta_3)$$

$$+\ m_3I_3l_2c_3\sin\theta_2\sin(\theta_2 + \theta_3)$$

$$+\ m_3^2l_2^2c_3^2\sin0_3\cos6_3\ \}$$

$$+\dot\theta_2^2\{m_3l_2c_3(2m_3l_2c_3\sin\theta_3 + I_2 + I_3 + m_3l_2^2)\}\cos\theta_3$$

$$+\dot\theta_3^2\{m_3l_2c_3(m_3l_2c_3\sin\theta_3 + I_3)\}\cos\theta_3$$

$$+\dot\theta_2\dot\theta_3\{2m_2l_2C + 2m_\wedge c_3^2\sin\theta\}\cos\theta \tag{3}$$

The robot model thus derived is highly coupled and non-linear, and all the coefficients are time variant. It is felt that unless this model is simplified greatly, there is little hope to extract any general information about the robot manipulator system. The next step therefore, is model reduction.

4 MODEL REDUCTION

The robot model is reduced by two schemes; (1) gravitational force compensation and (2) decoupling the waist rotation from the rest of the system. These are as follows;

(a) Gravitational force compensation

The (static) torque required for each rotary joint to hold the robot at any stand-still posture can be pre-calculated and stored in the robot contoi memory, ideally in a data base. To be specific the static torques are (from equation 1):

$$T1s = 0 \quad \text{(For any } 9\ ^\wedge$$

$$T2s = m_3g[l_2\cos6_2 + c_3\sin(0_2 + 0_3)] + m_2g\ c_2\cos0_2$$

$$T3s = m_3c_3g\ \sin(©_2\text{-i-}0_3)$$

Upon motion, the DBMS retrieves the value of the static torque required for its instantaneous position along the path of motion. The robot controller, on- the other hand, is to calculate the additional (dynamic) torque which is responsible for the arm. motion as well as the gripper loading

effect. The sum of these two is the total torque which is sent to the actuator and then to the rotary joint, Figure 5. If the gravitational force data base is considered an integral part of the robot system, then the total torque can be expressed as follows:

$$T1 = T1d$$

$$T2 = T2d + T2s$$
$$= T2d + m_3 g[l_2 \cos\Theta_2 + c_3 \sin(\Theta_2 + \Theta_3)] + m_2 g\, c_2 \cos\Theta_2$$

$$T3 = T3d + T3s$$
$$= T3d + m_3 c_3 g\, \sin(\Theta_2 + \Theta_3)$$

By substituting these transformations into equation1, the model equations can be simplified to the following form;

$$\{I_1 + m_2 l_1^2 + m_3 l_1^2 + I_3 \sin^2(\Theta_2 + \Theta_3) + (I_2 + m_3 l_2^2)\cos^2\Theta_2$$

$$+ 2l_1(m_2 c_2 + m_3 l_2)\cos\Theta_2 + 2m_3 l_1 c_3 \sin(\Theta_2 + \Theta_3)$$

$$+ 2m_3 l_2 c_3 \cos\Theta_2 \sin(\Theta_2 + \Theta_3) \quad\}\ddot\Theta_1 = T1d +$$

$$\dot\Theta_1 \dot\Theta_2 \{2[m_2 l_1 c_2 + m_3 l_1 l_2 + (I_2 + m_3 l_2^2)\cos\Theta_2]\sin\Theta_2$$

$$-2m_3 l_2 c_3[\cos\Theta_2 \cos(\Theta_2 + \Theta_3) - \sin\Theta_2 \sin(\Theta_2 + \Theta_3)]$$

$$-2[m_3 l_1 c_3 + I_3 \sin(\Theta_2 + \Theta_3)]\cos(\Theta_2 + \Theta_3) \quad\}-$$

$$\dot\Theta_1 \dot\Theta_3 \{2m_2 c_3(l_2 \cos\Theta_2 + l_1)\cos(\Theta_2 + \Theta_3) + 2I_3 \sin(\Theta_2 + \Theta_3)\cos(\Theta_2 + \Theta_3)\} \tag{4}$$

$$\{(I_2 + m_3 l_2^2)I_3 - m_3^2 l_2^2 c_3^2 \sin^2\Theta_3\}\ddot\Theta_2 = I_3 T2d - (I_3 + m_3 l_2 c_3 \sin\Theta_3)T3d$$

$$-\dot\Theta_1^2\{[m_2 I_3 l_1 l_2 + m_3 I_3 l_1 l_2 + (I_2 I_3 + m_3 I_3 l_2^2)\cos\Theta_2 + m_3 I_3 l_2 c_3 \sin(\Theta_2 + \Theta_3)]\sin\Theta_2$$

$$+ [m_3^2 l_1 l_2 c_3^2 + m_3^2 l_2^2 c_3^2 \cos\Theta_2 + m_3 I_3 l_2 c_3 \sin(\Theta_2 + \Theta_3)\sin\Theta_3 \cos(\Theta_2 + \Theta_3) \quad\}$$

$$-\dot\Theta_2^2\{m_3 l_2 c_3(I_3 + m_3 l_2 c_3 \sin\Theta_3)\cos\Theta_3\}$$

$$-\dot\Theta_3^2\{m_3 I_3 l_2 c_3 \cos\Theta_3\}$$

$$-\dot\Theta_2 \dot\Theta_3\{2m_3 I_3 l_2 c_3 \cos\Theta_3\} \tag{5}$$

$$\{(I_2 + m_3 l_2^2)I_3 - m_3^2 l_2^2 c_3^2 \sin^2\Theta_3\}\ddot\Theta_3 = \{-(I_3 + m_3 l_2 c_3 \sin\Theta_3)\}T2d$$

$$+ \{I_2 + I_3 + m_3 l_2^2 + 2m_3 l_2 c_3 \sin\Theta_3\}T3d$$

$$+ \dot\Theta_1^2\{[m_2 I_3 l_1 c_2 + m_3 I_3 l_1 l_2 + (I_2 I_3 + m_3 I_3 l_2^2)\cos\Theta_2 + m_2 m_3 l_1 l_2 c_2 c_3 \sin\Theta_3$$

$$+ m_3^2 l_1 l_2^2 c_3 \sin\Theta_3 + m_3 I_2 l_2 c_3 \sin\Theta_3 \cos\Theta_2 + m_3^2 l_2^3 c_3 \sin\Theta_3 \cos\Theta_2] \sin\Theta_2$$

$$+ [m_3^2 l_1 l_2 c_3^2 \sin\Theta_3 + (I_2 I_3 + m_3 I_3 l_2^2 + m_3 I_3 l_2 c_3 \sin\Theta_3) \sin(\Theta_2 + \Theta_3)$$

$$+ m_3 I_2 l_1 c_3 + m_3 I_2 l_2 c_3 \cos\Theta_2 + m_3^2 l_1 l_2^2 c_3 + m_3^2 l_2^3 c_3 \cos\Theta_2] \cos(\Theta_2 + \Theta_3)$$

$$+ m_3 I_3 l_2 c_3 \sin\Theta_2 \sin(\Theta_2 + \Theta_3)$$

$$+ m_3^2 l_2^2 c_3^2 \sin\Theta_3 \cos\Theta_3 \}$$

$$+ \dot{\Theta}_2^2 \{ m_3 l_2 c_3 (2 m_3 l_2 c_3 \sin\Theta_3 + I_2 + I_3 + m_3 l_2^2) \} \cos\Theta_3$$

$$+ \dot{\Theta}_3^2 \{ m_3 l_2 c_3 (m_3 l_2 c_3 \sin\Theta_3 + I_3) \} \cos\Theta_3$$

$$+ \dot{\Theta}_2 \dot{\Theta}_3 \{ 2 m_3 I_3 l_2 c_3 + 2 m_3^2 l_2^2 c_3^2 \sin\Theta_3 \} \cos\Theta_3 \tag{6}$$

(b) Decoupling the waist rotation from the rest of the system

In order to simplify the model equations further, the rotation about the first axis is decoupled from the rest of the system. To be specific;

When $\dot{\Theta}_1 \neq 0$, then $\dot{\Theta}_2 = \dot{\Theta}_3 = 0$

When $\dot{\Theta}_2$ or $\dot{\Theta}_3 \neq 0$, then $\dot{\Theta}_1 = 0$

While this appears arbitrary at the first sight, it smoothes the load to the actuator system. When all the rotary joints are moving simultaneously, a higher power demand will be required. Thus the decoupling may produce a smoother load profile such that the actuator system can be made smaller and cheaper as well as more energy efficient. The saving is particularly significant for the hydraulic type actuator systems. Besides, in gross motion there are very few tasks that cannot be accomplished by simple rotations and simple reaching. In this case, the model can be further reduced to the following form;

$$\{ I_1 + m_2 l_1^2 + m_3 l_1^2 + I_3 \sin^2(\Theta_2 + \Theta_3) + (I_2 + m_3 l_2^2) \cos^2\Theta_2$$

$$+ 2l_1 (m_2 c_2 + m_3 l_2) \cos\Theta_2 + 2 m_3 l_1 c_3 \sin(\Theta_2 + \Theta_3)$$

$$+ 2 m_3 l_2 c_3 \cos\Theta_2 \sin(\Theta_2 + \Theta_3) \qquad \} \ddot{\Theta}_1 = T1d \tag{7}$$

$$\{ (I_2 + m_3 l_2^2) I_3 - m_3^2 l_2^2 c_3^2 \sin^2\Theta_3 \} \ddot{\Theta}_2 = I_3 T2d - (I_3 + m_3 l_2 c_3 \sin\Theta_3) T3d$$

$$- \dot{\Theta}_2^2 \{ m_3 l_2 c_3 (I_3 + m_3 l_2 c_3 \sin\Theta_3) \cos\Theta_3 \}$$

$$- \dot{\Theta}_3^2 \{ m_3 I_3 l_2 c_3 \cos\Theta_3 \}$$

$$- \dot{\Theta}_2 \dot{\Theta}_3 \{ 2 m_3 I_3 l_2 c_3 \cos\Theta_3 \} \tag{8}$$

$$\{(I_2 + m_3 l_2^2)I_3 - m_3^2 l_2^2 c_3^2 \sin^2\Theta_3\}\ddot{\Theta}_3 = \{-(I_3 + m_3 l_2 c_3 \sin\Theta_3)\}T2d$$

$$+ \{I_2 + I_3 + m_3 l_2^2 + 2m_3 l_2 c_3 \sin\Theta_3\}T3d$$

$$+ \dot{\Theta}_2^2\{m_3 l_2 c_3(2m_3 l_2 c_3 \sin\Theta_3 + I_2 + I_3 + m_3 l_2^2)\}\cos\Theta_3$$

$$+ \dot{\Theta}_3^2\{m_3 l_2 c_3(m_3 l_2 c_3 \sin\Theta_3 + I_3)\}\cos\Theta_3$$

$$+ \dot{\Theta}_2\dot{\Theta}_3\{2m_3 I_3 l_2 c_3 + 2m_3^2 l_2^2 c_3^2 \sin\Theta_3\}\cos\Theta_3 \qquad (9)$$

After adopting these schemes, and applying the following change of variables;

$$X_1 = \dot{\Theta}_1$$

$$X_2 = \dot{\Theta}_2$$

$$X_3 = (\dot{\Theta}_2 + \dot{\Theta}_3)$$

Then, the model equations are in very simple form (Figure 3 and equations below)

$$\{I_1 + m_2 l_1^2 + m_3 l_1^2 + I_3 \sin^2(\Theta_2 + \Theta_3) + (I_2 + m_3 l_2^2)\cos^2\Theta_2$$

$$+ 2l_1(m_2 c_2 + m_3 l_2)\cos\Theta_2 + 2m_3 l_1 c_3 \sin(\Theta_2 + \Theta_3)$$

$$+ 2m_3 l_2 c_3 \cos\Theta_2 \sin(\Theta_2 + \Theta_3) \qquad \}\dot{X}_1 = T1d \qquad (10)$$

$$\{(I_2 + m_3 l_2^2)I_3 - m_3^2 l_2^2 c_3^2 \sin^2\Theta_3\}\dot{X}_2 = I_3 T2d - (I_3 + m_3 l_2 c_3 \sin\Theta_3)T3d$$

$$- X_2^2(m_3^2 l_2^2 c_3^2 \sin\Theta_3 \cos\Theta_3]$$

$$- X_3^2(m_3 I_3 l_2 c_3 \cos\Theta_3) \qquad (11)$$

$$\{(I_2 + m_3 l_2^2)I_3 - m_3^2 l_2^2 c_3^2 \sin^2\Theta_3\}\dot{X}_3 = \{-(m_3 l_2 c_3 \sin\Theta_3)\}T2d + \{I_2 + m_3 l_2^2 + m_3 l_2 c_3 \sin\Theta_3\}T3d$$

$$+ \{I_2 + m_3 l_2^2 + m_3 l_2 c_3 \sin\Theta_3\}T3d$$

$$+ X_2^2[m_3 l_2 c_3(I_2 + m_3 l_2^2)\cos\Theta_3]$$

$$+ X_3^2[m_3^2 l_2^2 c_3^2 \sin\Theta_3 \cos\Theta_3] \qquad (12)$$

The robot model just derived is still non-linear, coupled, and time-varing. However, due to its simplicity, an analytical approach is possible. Through this attempt some general conclusions may be reached and are applicable to other similar robots. One accredited contribution of this model is that it cuts down the cost of computer simulation.

5 CONCLUDING REMARKS

An interesting observation can be reported at this moment. If C3 is designed to be zero by a counter weight on the third link then the model equations can be put into an even simpler form.

$$\{I_1 + m_2 l_1^2 + m_3 l_1^2 + I_3 \sin^2(\Theta_2 + \Theta_3) + (I_2 + m_3 l_2^2)\cos^2\Theta_2 +$$

$$2(m_2 l_1 c_2 + m_3 l_1 l_2)\cos\Theta_2\}\ddot{\Theta}_1 = T1d \tag{13}$$

$$\{(I_2 + m_3 l_2^2)I_3\}\ddot{\Theta}_2 = I_3 T2d - I_3 T3d \tag{14}$$

$$\{(I_2 + m_3 l_2^2)I_3\}\ddot{\Theta}_3 = -I_3 T2d + (I_2 + I_3 + m_3 l_2^2)T3d \tag{15}$$

In this last version, the robot equations are linear, completely decoupled from each other, and with constant coefficients (except that for the waist rotation). This linear model is invaluable for the future system analysis. The current research work seems to suggest a balanced design for the third link, and it should be built massively to offset the gripper loading effect. Ongoing work is concerned with data collection of the gripper loads during the manipulation of turbine blades being manufactured in a flexible manufacturing cell. Once the spectrum of activities has been identified proposed modifications to the arm design can proceed. The result of such modifications will be a robotic manipulator with greater positional accuracy.

REFERENCES

[1]   Young, J.F., "Robotics". Butterworths, London (1973).

[2]   Potter, R.D., "Practical Applications of a Limited Sequence Robot". Proc. 5th International Symposium of Industrial Robots. September 22-24, 1975.

[3]   Nevins, J. L., Whitney, D.E., "Adaptable Programmable Assembly Systems: An Information and Control Problem". Proc. 5th International Symposium on Industrial Robots. September 22-24, 1975.

[4]   Corwin, M., "The Benefits of a Computer Controlled Robot". Proc. 5th International Symposium on Industrial Robots. September 22-24, 1975.

[5]   Cunningham, C.S., "Robot Flexibility Through Software". Proc. 9th International Symposium on Industrial Robots. March 13-15, 1979.

[6]   Whitney, D.E., "The Mathematics of Coordinated Control of Prosthetic Arms and Manipulators". Trans. ASME. J. of Dynamic Systems, Measurement and Control. December 1972.

[7]   Paul, R.L., "Manipulator Path Control". Proc. International Conference on Cybernetics and Society. Setember 23-25, 1975.

[8]   Pieper, D.L., Roth, B., "The Kinematics of Manipulators under Computer Control". Ph.D. Thesis, Stanford University. October, 1968.

[9]   Albus, J.S., "A New Approach to Manipulator Control: The Cerebellar Modal Articulation Controller (CACM)". Trans. ASME J. of Dynamic Systems, Measurement and Control. September, 1975.

[10]   Anderson, T.R., Paul, R.L., "High Speed Coordinated Control of Industrial Robots". Proc. 9th International Symposium on Industrial Robots. March 13-15, 1979.

[11]   Klein, C.A., Maney, J.J., "Real-Time Control of a Multiple Element Mechanical Linkage With a Microcomputer". Trans. IEEE Industrial Electronics and Control Instrumentation, Vol. 26, No. 4. November, 1979.

[12]   Dubowsky, S., DesForge, D.T., "The Application of Model Reference Adaptive Control to Robotic Manipulators". Trans. ASME J. of Dynamic Systems, Measurement and Control. September, 1979.

[13]   Kahn, M.E., Roth, B., "The Near Minimum-Time Control of Open-Loop Articulated Kinematic Chains". Trans. ASME J. of Dynamic Systems, Measurement and Control. September, 1971.

[14]   Donalson, D.D., Leondes, C.T., "A Model Referenced Parameter Tracking Technique for Adaptive Control Systems: Part 1- The Principles of Adaptation and Part 2- Stability Analysis by the Second Method of Lyapunov". Trans. IEEE Applications and Industry, Vol. 82, No. 68. September, 1963.

APPENDIX A

The general kinematic equations for relative motions in a moving reference frame are (figure A-1):

$$\vec{R}_b = \vec{R}_a + \vec{w} \times \vec{\rho}_B + \dot{\vec{\rho}}_B$$

$$\ddot{\vec{R}}_b = \ddot{\vec{R}}_a + \vec{w} \times (\vec{w} \times \vec{\rho}_B) + \dot{\vec{w}} \times \vec{\rho}_B + 2\vec{w} \times \dot{\vec{\rho}}_B + \ddot{\vec{\rho}}_B$$

Such equations state that:

$$\begin{pmatrix} \text{absolute velocity} \\ \text{of point B} \end{pmatrix} = \begin{pmatrix} \text{absolute velocity} \\ \text{of point A} \end{pmatrix} + \begin{pmatrix} \text{relative velocity} \\ \text{of B to A} \end{pmatrix}$$

$$\begin{pmatrix} \text{absolute} \\ \text{accel. of} \\ \text{point B} \end{pmatrix} = \begin{pmatrix} \text{absolute} \\ \text{accel. of} \\ \text{point A}\cdot \end{pmatrix} + \begin{pmatrix} \text{relative} \\ \text{accel. of} \\ \text{B to A} \end{pmatrix} + \begin{pmatrix} \text{Coriolis} \\ \text{terms} \end{pmatrix}$$

For the robot under consideration, the relative motion is caused by a rotation with respect to the moving frame. For clarity, the absolute acceleration of each rotary joint is determined first; (Figure 4)

$$a_{j1} = 0$$

$$a_{j2} = l_1\ddot{\theta}_1\vec{i}_\theta - l_1\dot{\theta}_1^2\vec{i}_r$$

$$a_{j3} = (l_2\ddot{\theta}_2\cos\theta_2 - l_2\dot{\theta}_2^2\sin\theta_2)\vec{i}_z$$

$$\quad -(l_1\dot{\theta}_1^2 + l_2\dot{\theta}_1^2\cos\theta_2 + l_2\ddot{\theta}_2\sin\theta_2 + l_2\dot{\theta}_2^2\cos\theta_2)\vec{i}_r$$

$$\quad + (l_1\ddot{\theta}_1 + l_2\ddot{\theta}_1\cos\theta_2 - 2l_2\dot{\theta}_1\dot{\theta}_2\sin\theta_2)\vec{i}_\theta$$

For any point P on the third link, the absolute acceleration of P can be found by applying the general kinematic equation. The rotation of the moving frame is composed of two components, one to the Z axis, the other to the -θ axis. (Figure A-2)

$$a_{p3} = a_{j3} + \text{ relative acceleration of point P}$$
$$\quad\quad\quad\quad \text{with respect to the rotary joint j3}$$

$$= a_{j3} + X_3\sin(\theta_2 + \theta_3)\ddot{\theta}_1\vec{i}_\theta \quad\quad\quad (\text{due to } \ddot{\theta}_1)$$

$$\quad -X_3\sin(\theta_2 + \theta_3)\dot{\theta}_1^2\vec{i}_r \quad\quad\quad\quad (\text{due to } \dot{\theta}_1)$$

$$\quad + X_3(\ddot{\theta}_2 + \ddot{\theta}_3)\sin(\theta_2 + \theta_3)\vec{i}_z \quad\quad (\text{due to } \ddot{\theta}_2 + \ddot{\theta}_3)$$

$$\quad + X_3(\ddot{\theta}_2 + \ddot{\theta}_3)\cos(\theta_2 + \theta_3)\vec{i}_r \quad\quad (\text{due to } \ddot{\theta}_2 + \ddot{\theta}_3)$$

$$+ X_3(\dot{G}_2 + \dot{9}_3)^2\cos(e_2 + 9_3)\vec{i}_z \qquad \text{(due to } \dot{9}_2 + \dot{9}_3)$$

$$-X_3(\dot{G}_2 + \dot{e}_3)^2\sin(9_2 + 9_3)f_r \qquad \text{(due to } \dot{9}_2 + \dot{9}_3)$$

$$+ 2X39^\wedge\dot{9}_{.,} + 9_3)\cos(9_2 + 9_3)i_e \qquad \text{(Coriolis term)}$$

$$= \vec{i}_e p_1 + l_2\cos9_2 + X_3\sin(9_2 + 9_3)]\ddot{9}_1$$

$$+1_r[X_3(\ddot{9}_2 + \ddot{9}_3)\cos(9_2 + 9_3)-X_3(\dot{9}_2 + \dot{9}_3)^2\sin(9_2 + 9_3)-X_39_1^2\sin(9_2 + 9_3)$$

$$-l_i\dot{e}_1^2-l_29^2\cos9_2-l_2\ddot{9}_2\sin e_2-l_29^2_{2c}os9_2]$$

$$+\vec{i}_z[X_3(\ddot{9}_2 + \ddot{9}_3)\sin(9_2 + 9_3) + X_3(\dot{9}_2 + \dot{9}_3)^2\cos(9_2 + 9_3) + l_2\ddot{9}_2\cos9_2$$

$$-l_29^2_2\sin9_2]7_z$$

$$+ \vec{i}_Q[2X_3\dot{9}_1(\dot{9}_2 + \dot{9}_3)\cos(9_2 + 9_3)-2l_2\dot{9}_1\dot{9}_2\sin9_2]$$

By the same procedure, the absolute acceleration of any point P on the second or on the first link can be found to be (Figure A-2):

$$a_{p2} = i_e[(X_2\cos9_2 + l^\wedge\ddot{e}_1-2X_2\dot{\Theta}_1\Theta_2\sin\Theta_2]$$

$$-\vec{i}_r[X_2\dot{\Theta}_1^2\cos\Theta_2 + X_2\ddot{9}_2\sin9_2 + X_2\dot{9}_2^2\cos9_2 + {}^\wedge\dot{G}_1^2]$$

$$+ \vec{i}_z p<_2\ddot{9}_2\cos9_2-X_2\dot{9}^\wedge\sin9_2]$$

$$\mathbf{a_{p1}} = X_1\ddot{\Theta}_1\vec{i}_\Theta-X_1\dot{\Theta}_1^2\vec{i}_r$$

Once the absolute acceleration is known, then the D'Alembert principle can be applied.

APPENDIX B

The equations of motion are derived in a reverse order, the third link first, then the second link, and then the first link. The general procedure in deriving these equations are:

1. Find the sum of the inertia force to the local coordinate axis

2. Find the sum of moment by the inertia force to the rotary joint

3. Write equilibrium equations and solve them

For the third link, the sum of inertia force can be found as follows:

$$\vec{F}_R = (\vec{i}_r) \int [-\vec{a}_{p3} \cdot \vec{i}_r] \cdot dm_3$$

$$= (\vec{i}_r) \int (-1)[X_3(\ddot{\Theta}_2 + \ddot{\Theta}_3)\cos(\Theta_2 + \Theta_3) - X_3(\dot{\Theta}_2 + \dot{\Theta}_3)^2\sin(\Theta_2 + \Theta_3)$$

$$-X_3\dot{\Theta}_1^2\sin(\Theta_2 + \Theta_3) - l_1\dot{\Theta}_1^2 - l_2\dot{\Theta}_1^2\cos\Theta_2$$

$$-l_2\ddot{\Theta}_2\sin\Theta_2 - l_2\dot{\Theta}_2^2\cos\Theta_2]dm_3$$

$$= \vec{i}_r[m_3\dot{\Theta}_1^2(l_1 + l_2\cos\Theta_2 + c_3\sin(\Theta_2 + \Theta_3))$$

$$+ m_3c_3((\dot{\Theta}_2 + \dot{\Theta}_3)^2\sin(\Theta_2 + \Theta_3) - (\ddot{\Theta}_2 + \ddot{\Theta}_3)\cos(\Theta_2 + \Theta_3))$$

$$+ m_3l_2(\ddot{\Theta}_2\sin\Theta_2 + \dot{\Theta}_2^2\cos\Theta_2) \qquad]$$

$$\vec{F}_\Theta = \vec{i}_\Theta \int [-\vec{a}_{p3} \cdot \vec{i}_\Theta]dm_3$$

$$= \vec{i}_\Theta[-m_3l_1\ddot{\Theta}_1 - m_3l_2\ddot{\Theta}_1\cos\Theta_2 - m_3c_3\ddot{\Theta}_1\sin(\Theta_2 + \Theta_3) - 2m_3c_3\dot{\Theta}_1(\dot{\Theta}_2 + \dot{\Theta}_3)\cos(\Theta_2 + \Theta_3)$$

$$+ 2m_3l_2\dot{\Theta}_1\dot{\Theta}_2\sin\Theta_2]$$

$$\vec{F}_z = \vec{i}_z \int [-\vec{a}_{p3} \cdot \vec{i}_z]dm_3$$

$$= \vec{i}_z[m_3l_2(\dot{\Theta}_2^2\sin\Theta_2 - \ddot{\Theta}_2\cos\Theta_2) - m_3c_3((\ddot{\Theta}_2 + \ddot{\Theta}_3)\sin(\Theta_2 + \Theta_3) + (\dot{\Theta}_2 + \dot{\Theta}_3)^2\cos(\Theta_2 + \Theta_3))]$$

$$M = (-\vec{i}_\Theta)\{ \int [-\vec{a}_{p3} \cdot \vec{i}_r]X_3\cos(\Theta_2 + \Theta_3)dm_3 + \int [-\vec{a}_{p3} \cdot \vec{i}_z]X_3\sin(\Theta_2 + \Theta_3)dm_3\}$$

$$= -\vec{i}_\Theta\{I_3(\ddot{\Theta}_2 + \ddot{\Theta}_3) + I_3\dot{\Theta}_1^2\sin(\Theta_2 + \Theta_3)\cos(\Theta_2 + \Theta_3) + m_3c_3l_1\dot{\Theta}_1^2\cos(\Theta_2 + \Theta_3)$$

$$+ m_3c_3l_2[\dot{\Theta}_1^2\cos\Theta_2\cos(\Theta_2 + \Theta_3) - \ddot{\Theta}_2\sin\Theta_3 + \dot{\Theta}_2^2\cos\Theta_3]\}$$

The equilibrium equations are (Figure B-1):

$$\vec{R}_r + \vec{F}_r = 0$$

$$\vec{R}_z + \vec{F}_z - m_3\vec{g} = 0$$

$$\vec{M}_3 + \vec{T}_3 - m_3\vec{g}\, c_3\sin(\Theta_2 + \Theta_3) = 0$$

Solving for the unknown

$$\vec{R}_r = \vec{i}_r\{-m_3\dot{\Theta}_1^2[l_1 + l_2\cos\Theta_2 + c_3\sin(\Theta_2 + \Theta_3)]$$

$$-m_3c_3[(\dot{\Theta}_2 + \dot{\Theta}_3)^2\sin(\Theta_2 + \Theta_3) - (\ddot{\Theta}_2 + \ddot{\Theta}_3)\cos(\Theta_2 + \Theta_3)]$$

$$-m_3l_2[\ddot{\Theta}_2\sin\Theta_2 + \dot{\Theta}_2^2\cos\Theta_2]\qquad\}$$

$$\vec{R}_z = \vec{i}_z\{m_3g - m_3l_2(\dot{\Theta}_2^2\sin\Theta_2 - \ddot{\Theta}_2\cos\Theta_2)$$

$$+ m_3c_3[(\ddot{\Theta}_2 + \ddot{\Theta}_3)\sin(\Theta_2 + \Theta_3) + (\dot{\Theta}_2 + \dot{\Theta}_3)^2\cos(\Theta_2 + \Theta_3)]\}$$

$$\vec{T}_3 = -\vec{i}_\Theta\{m_3c_3g\,\sin(\Theta_2 + \Theta_3) - m_3c_3l_1\dot{\Theta}_1^2\cos(\Theta_2 + \Theta_3)$$

$$+ I_3(\ddot{\Theta}_2 + \ddot{\Theta}_3) - I_3\dot{\Theta}_1^2\sin(\Theta_2 + \Theta_3)\cos(\Theta_2 + \Theta_3)$$

$$- m_3c_3l_2[\dot{\Theta}_1^2\cos\Theta_2\cos(\Theta_2 + \Theta_3) - \ddot{\Theta}_2\sin\Theta_3 + \dot{\Theta}_2^2\cos\Theta_3]\}$$

The reactional force thus derived is to be used when writing the equilibrium equations for the second/first link.

By the same procedure, the equation of motion for the second link and for the first link can be expressed as follows:

$$T_2 + -\vec{i}_\Theta\{\ddot{\Theta}_2(I_2 + m_3c_3l_2\sin\Theta_3 + m_3l_2^2)$$

$$+ (\ddot{\Theta}_2 + \ddot{\Theta}_3)[I_3 + m_3c_3l_2\sin\Theta_3]$$

$$+ \dot{\Theta}_1^2[I_2\cos\Theta_2\sin\Theta_2 + m_2l_1c_2\sin\Theta_2 - I_3\sin(\Theta_2 + \Theta_3)\cos(\Theta_2 + \Theta_3)$$

$$- m_3c_3l_1\cos(\Theta_2 + \Theta_3) - m_3c_3l_2\cos\Theta_2\cos(\Theta_2 + \Theta_3)$$

$$+ m_3l_2\sin\Theta_2(l_1 + l_2\cos\Theta_2 + c_3\sin(\Theta_2 + \Theta_3)]$$

$$- \dot{\Theta}_2^2[m_3c_3l_2\cos\Theta_3]$$

$$+ m_3c_3l_2(\dot{\Theta}_2 + \dot{\Theta}_3)^2\cos\Theta_3$$

$$+ m_3g[l_2\cos\Theta_2 + c_3\sin(\Theta_2 + \Theta_3)] + m_2g\,c_2\cos\Theta_2\qquad\}$$

$$T_1 = \vec{i}_z\{\ddot{\Theta}_1[I_1 + m_2l_1^2 + m_3l_1^2 + (I_2 + m_3l_2^2)\cos^2\Theta_2$$

$$+ 2l_1(m_2c_2 + m_3l_2)\cos\Theta_2$$

$$+ I_3\sin^2(\Theta_2 + \Theta_3) + 2m_3l_1c_3\sin(\Theta_2 + \Theta_3)$$

$$+ 2m_3l_2c_3\cos\Theta_2\sin(\Theta_2 + \Theta_3)]$$

$$-\dot{\Theta}_1\dot{\Theta}_2[2(m_2 l_1 c_2 + m_3 l_1 l_2 + I_2 \cos\Theta + m_3 l_2^2 \cos\Theta_2)\sin\Theta_Z$$

$$-2m_3 l_2 c_3(\cos\Theta_2\cos(\Theta_2 + \Theta_3) - \sin(\Theta_2 + \Theta_3)\sin\Theta_2)$$

$$-2(m_3 l_1 c_3 + I_3 \sin(\Theta_2 + \Theta_3))\cos(\Theta_2 + \Theta_3) \qquad]$$

$$+ \dot{\Theta}_1\dot{\Theta}_3[2m_3 c_3(l_2\cos\Theta_2 + l_1)\cos(\Theta_2 + \Theta_3) + 2I_3\sin(\Theta_2 + \Theta_3)\cos(\Theta_2 + \Theta_3)]\}$$

Figu re 1: Different paths by servogains.

K_x -X axis servo gain, K_v - Y axis servo gain.
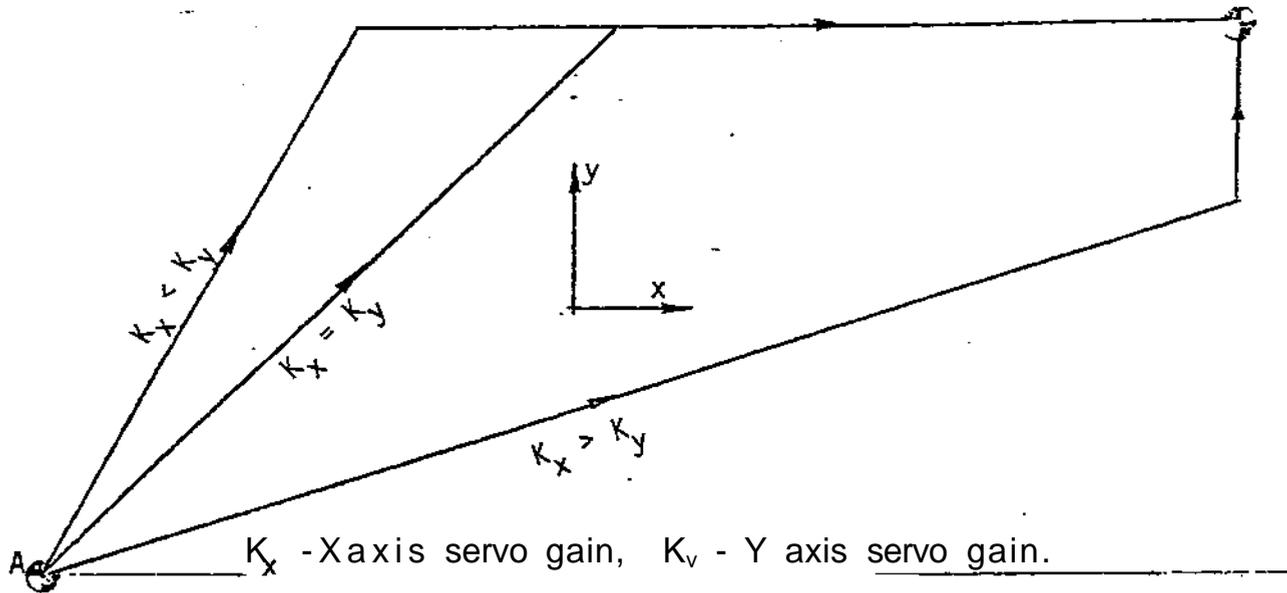
Figure 1. Different paths due to different servo gains.

Figure 2:
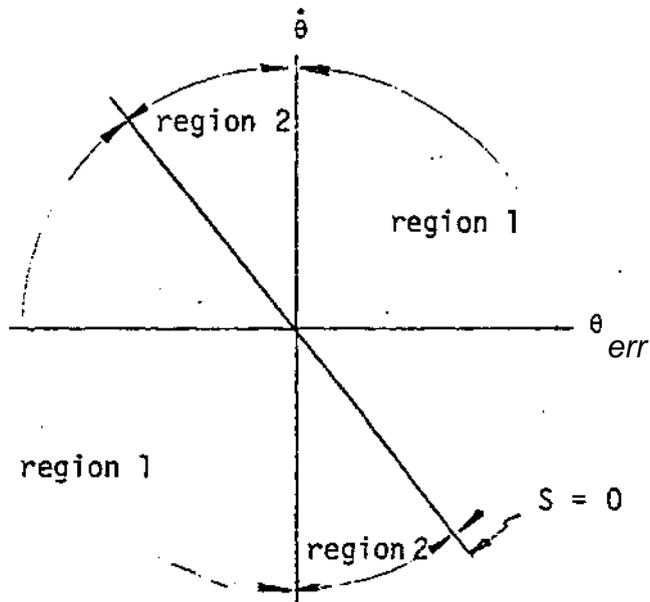
Figure 2-a.
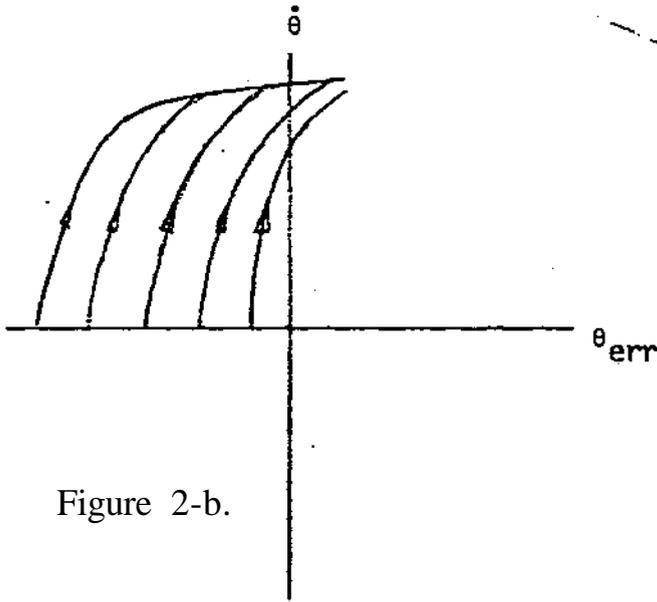
Figure 2-b.
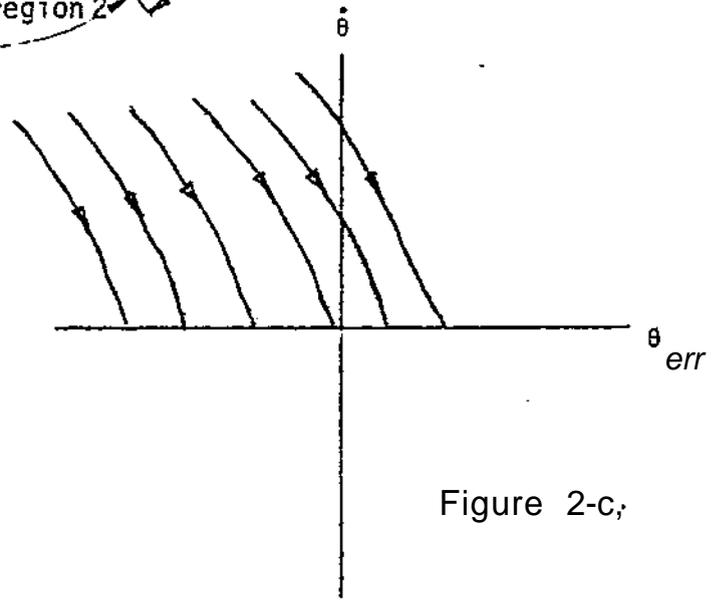
Figure 2-c.
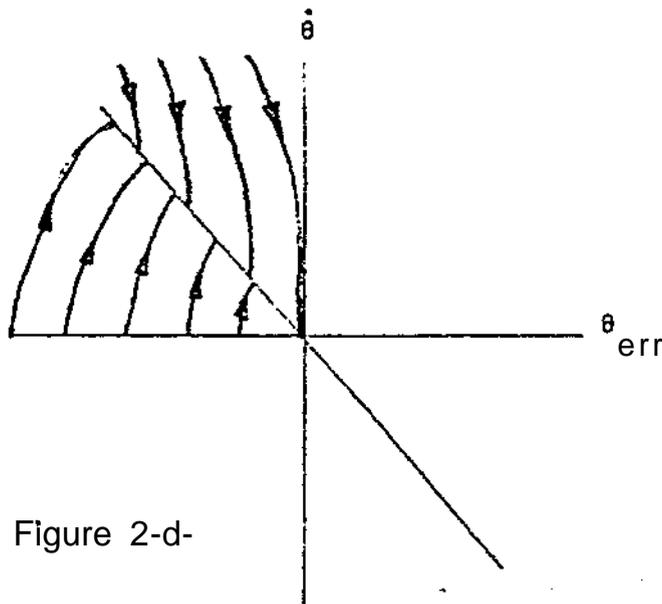
Figure 2-d-

Figu re 3: General model reference adaptive control system
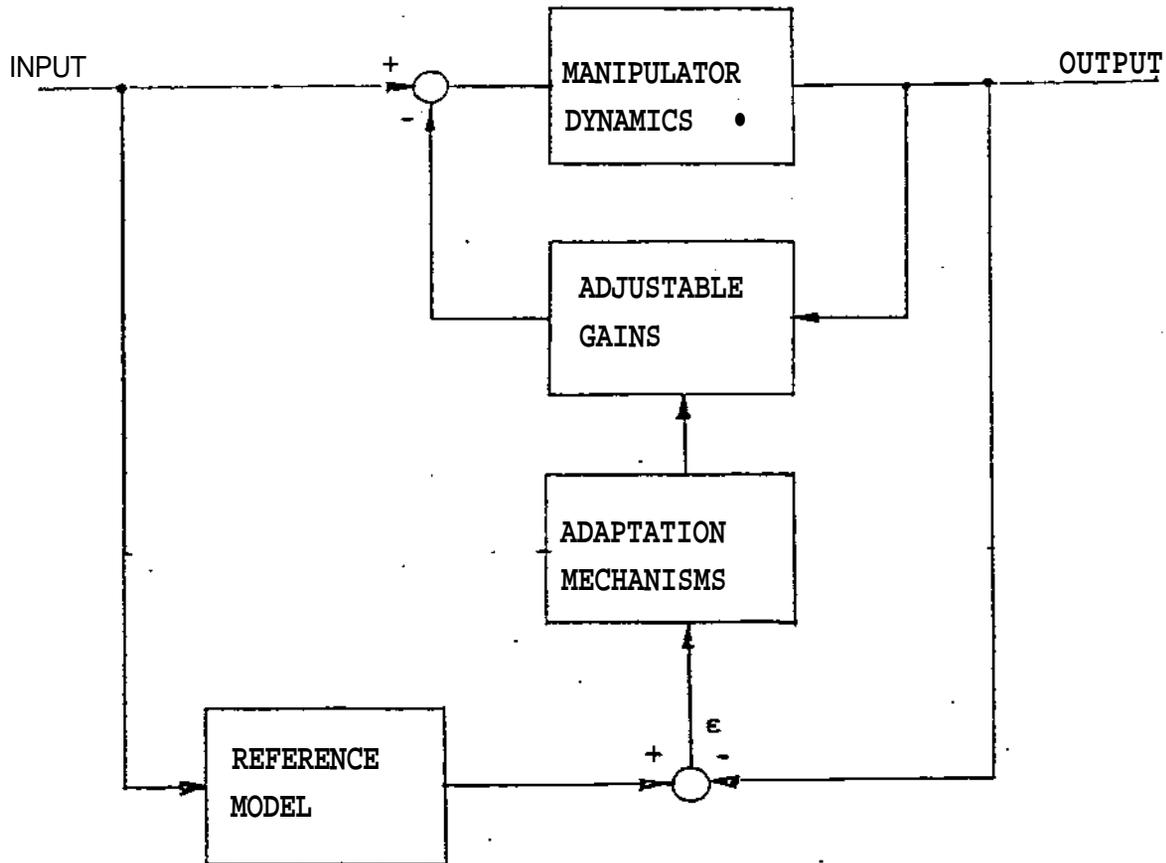
Figure 3- General model reference adaptive control system.

Figure 4: The Robot Schematic

3rd Link, with M_3, ℓ_3, I_3

2nd Link, with M_2, ℓ_2, I_2

1st Link, with M_1, ℓ_1, I_1

M: mass, ℓ: length, I: Moment of inertia
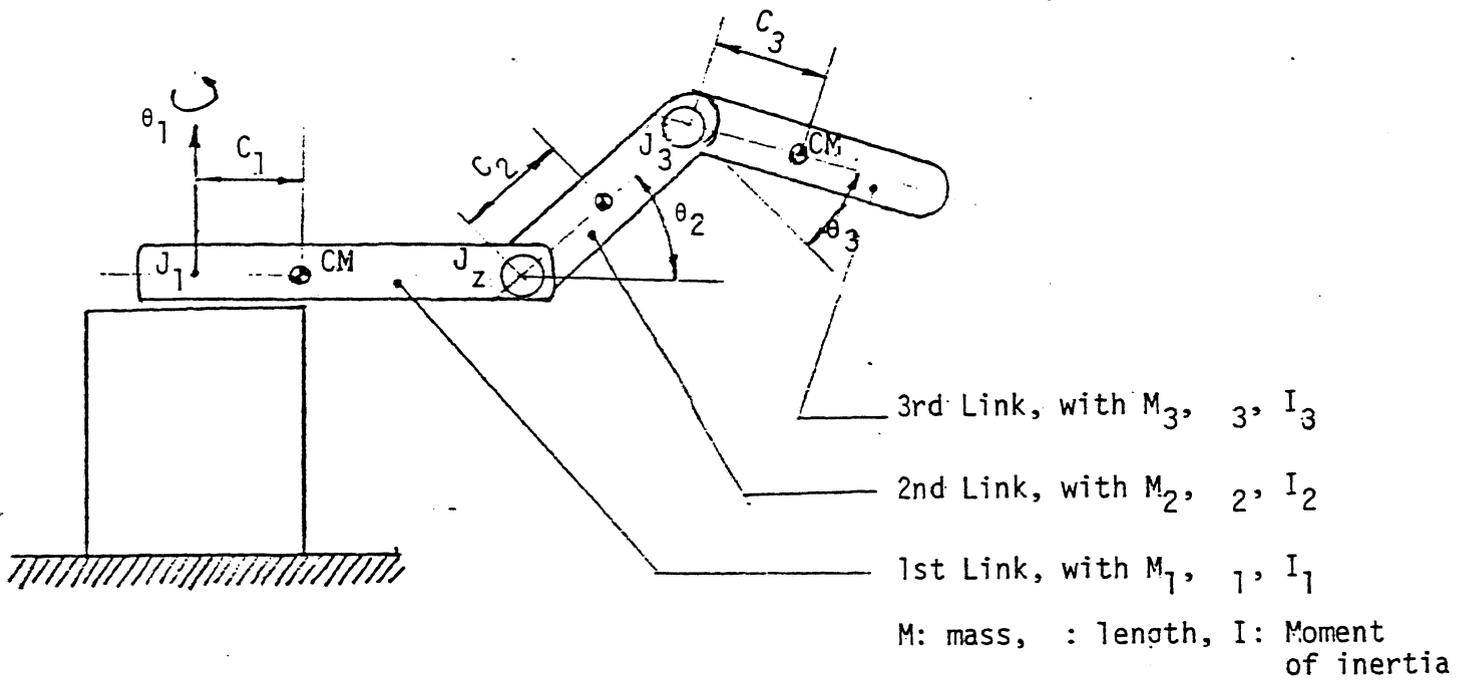
Figure 4. The robot schematic.

Figure 5: Gravitation force compensation.
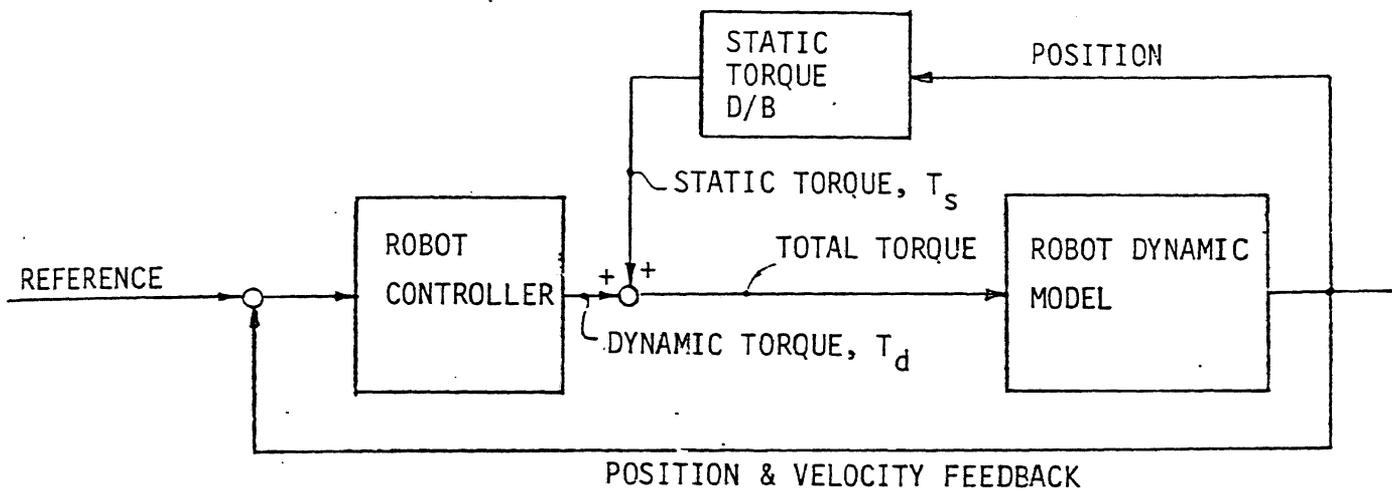
Figure 5. Gravitation force compensation.

Figure 6: The Robot Mode! After Reduction.
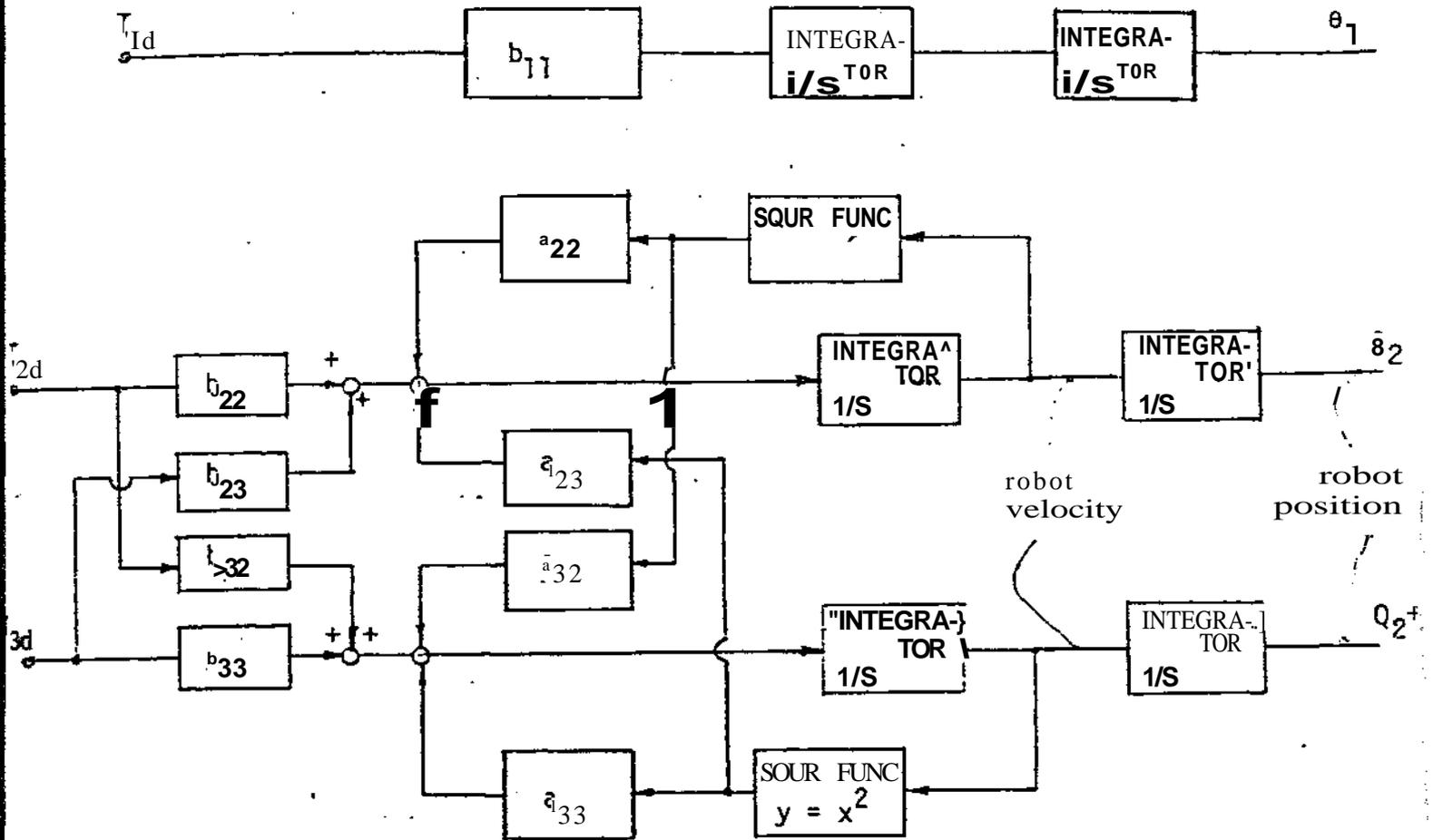
Figure 6. The robot model after reduction.

Figure 7: A1.
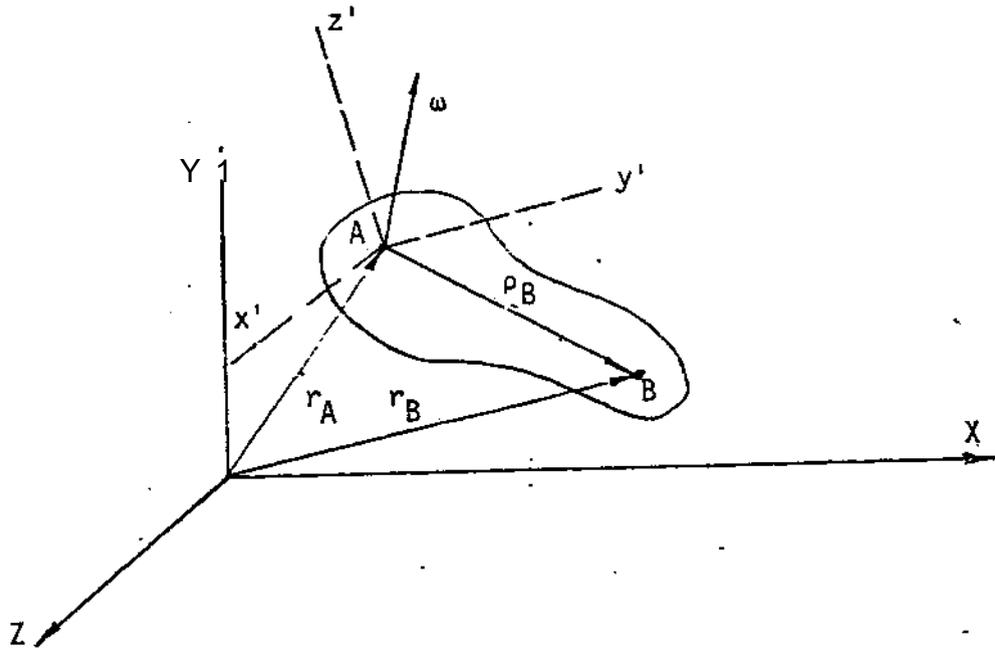
Figure A-I.
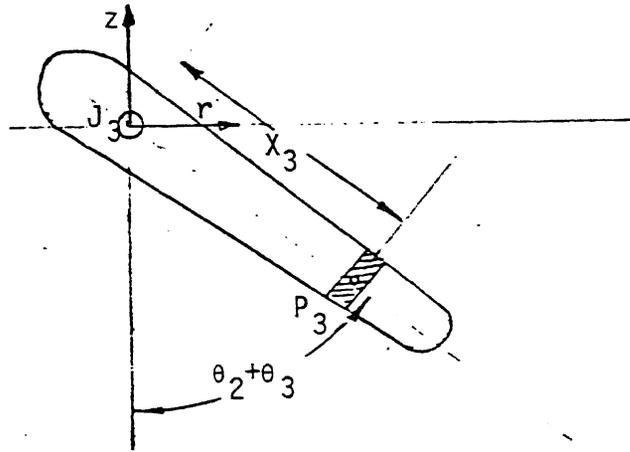
Figure A-2.   The 3rd link.

Figure 8: A2 - The 3rd Link
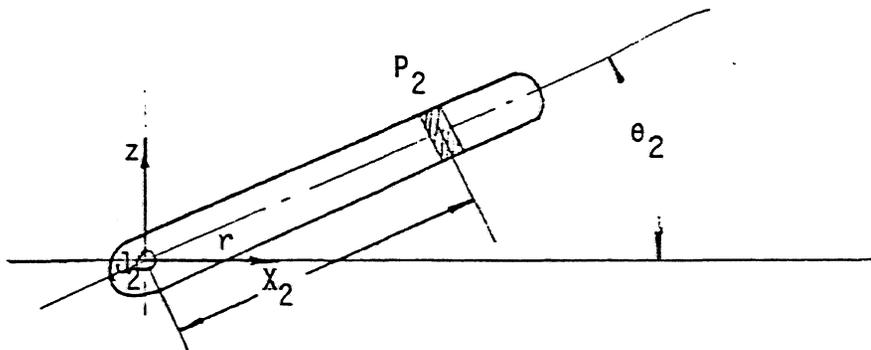
Figure A-3.   The 2nd link.

Figure 9: A3 - The 2nd Link

Figure 10: B1. Equilibrium of the 3rd Link.
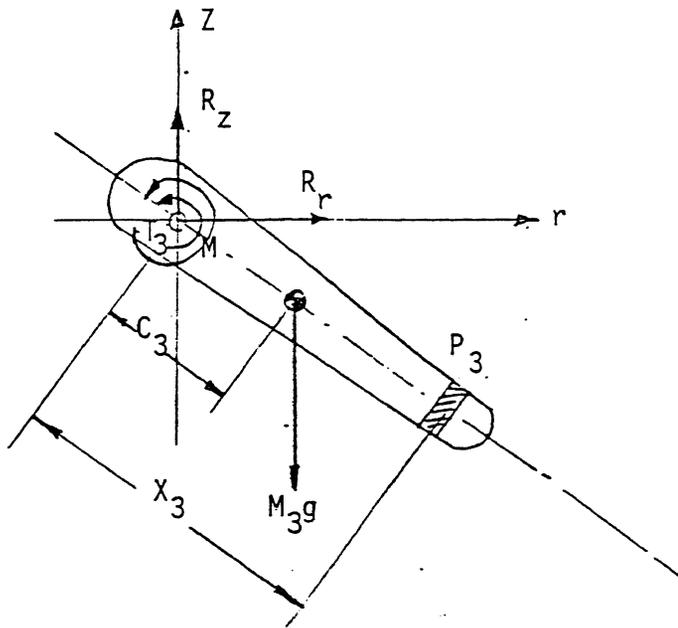
Figure B-1. Equilibrium of the 3rd link.